IJISET - International Journal of Innovative Science, Engineering & Technology, Vol. 3 Issue 3, March 2016.
www.ijiset.com
ISSN 2348 – 7968

Modelling Of Safa Reservoir Rock In Faghur – Siwa Basin, Western-Desert, Egypt

Abd-El-Gawad*, E. A., M. Fathy*, Abd-El-Dayem, Kh.**

* Geology Department, Faculty of Science, Al-Azhar University
**Egyptian General Petroleum Corporation.

Abstract

This study is aimed to assess the reservoir rock in Faghur-Siwa basin through the subsurface geological studies. These were made to show thickness variation, lithofacies changes and structural elements impacting the area. The different reservoir parameters evaluated to distinguish the pay zones for further exploration activities.

1. Introduction

The area under study is concerned with Faghur - Siwa basin oil field. It lies between Latitudes 25°00', 30°00' N and Longitudes 25°00' – 27°00' E (Fig.1). Faghur-Siwa basin is a north-south oriented Paleozoic basin covered wide stretches in the north western reaches of the Western Desert and can be regarded as a northern extension of Libya's Kufra Paleozoic basin. The Faghur-Siwa basin is a continental sag, craton interior basin, holds thick Paleogoic sequences, extending from Cambro-Ordovician to Carboniferous. Hydrocarbon source potential is proposed by some authors within limestones and shales of Carboniferous and Devonian. Recent discoveries in the Umbaraka area to the east are adjacent to, and probably aerated from, updipping Paleozoic potential sources in the Faghur-Siwa basin **(Schlumberger, 1995)**.

2. Stratigraphic Framework of the Western Desert

The stratigraphic column of the northern Western Desert is thick and embraces most of the sedimentary succession from Pre-Cambrian Basement Complex to Recent (Fig. 2).

ISSN 2348 – 7968

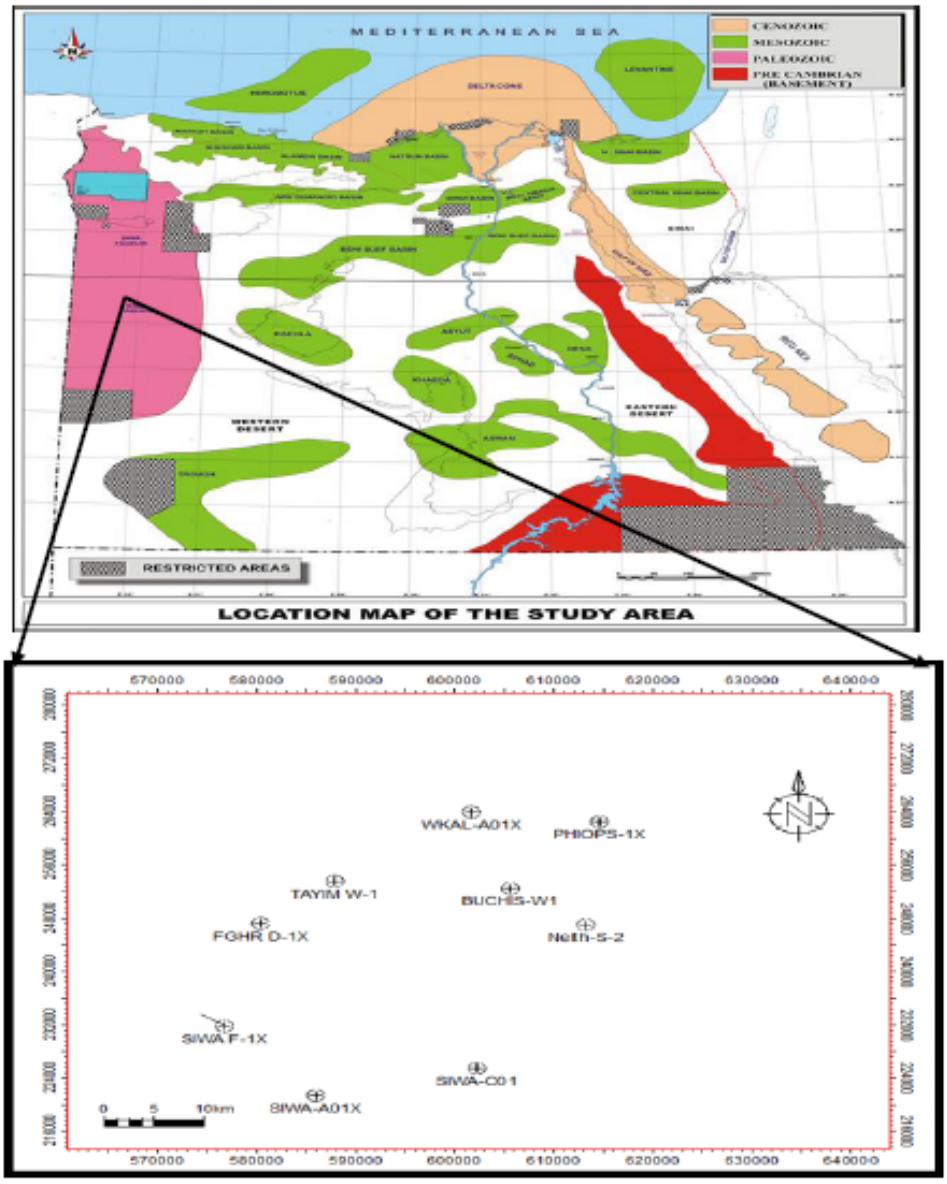

Fig. (1): Location map of the study area stating the location of the drilled wells in Faghur - Siwa Basin, North Western Desert, Egypt.

The total thickness, despite some anomalies, is raised progressively to the north and northeast from about 6000 ft. in the southern extends to about 25,000 ft. along the coastal area. The sedimentary section of the Western Desert varies from Lower Paleozoic to Resent. According to **Said (1990)** four major sedimentary cycles happened with comparable maximum southward transgression during the Carboniferous, Upper Jurassic, Middle and Late Cretaceous and Pliocene ages' times.

ISSN 2348 – 7968

Also, maximum north word regressive phases took place during Permo- Triassic and Early Jurassic and continued in the Early Cretaceous and again in the Late Eocene to Oligocene with final phase in the Late Miocene time.

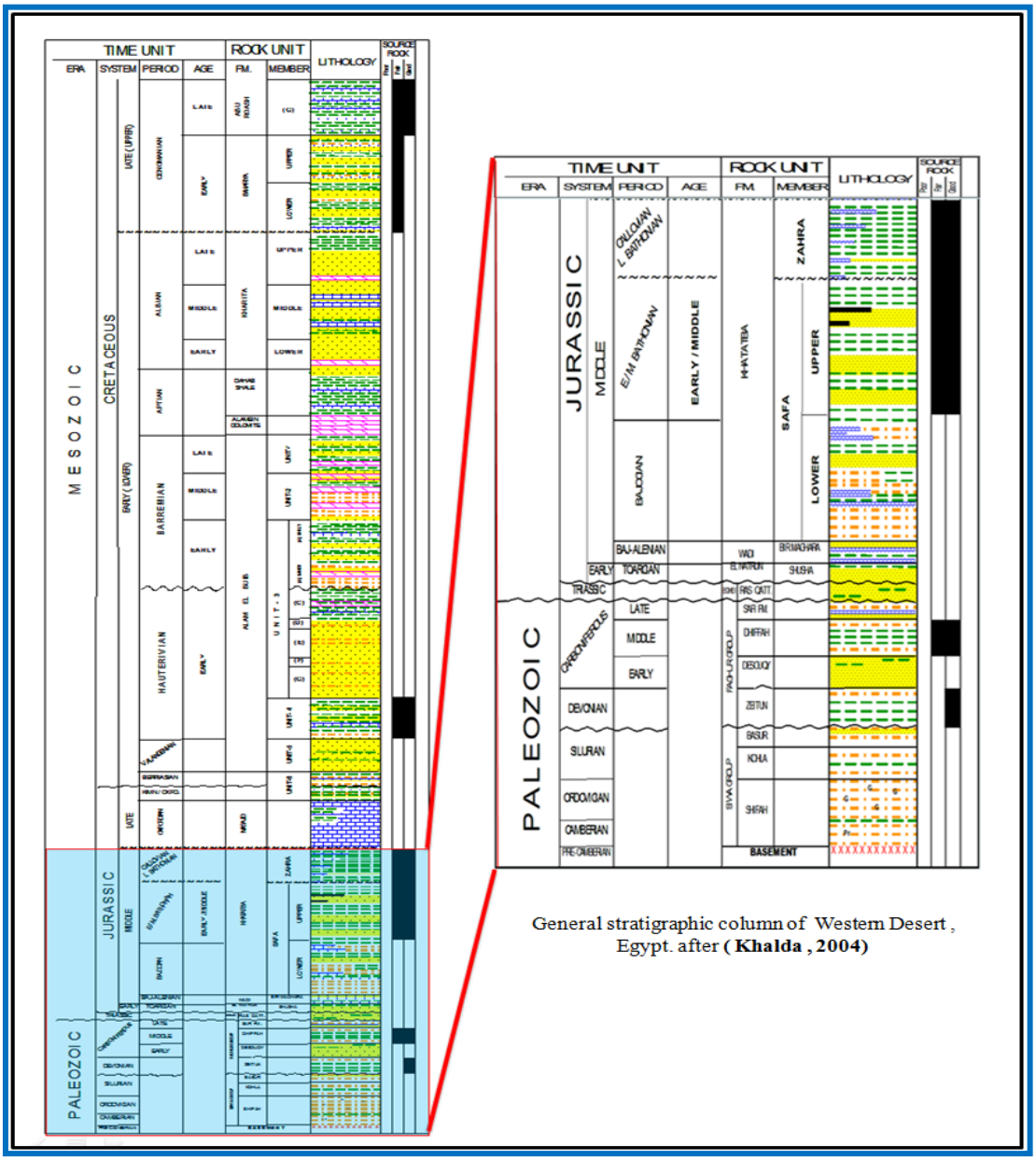

Fig. (2): Generalized stratigraphic column of the North Western Desert, **(Khalda, 2004)**

EGPC (1992) arranged subsurface lithostratigraphic column of the north Western Desert into five cycles from base to top as follows:

- A cycle of clastic facies controls the oldest sedimentary rocks and embraces the entire Paleozoic and Lower Jurassic formations.
- A carbonate section of middle and Upper Jurassic formations.
- A cycle of clastics contains the Lower Cretaceous up to the Upper Cretaceous (Early Cenomanian).
- From Upper Cenomanian and Upper to the Middle Eocene, carbonate deposits are again classified throughout northern Western Desert.
- The upper most clastic depositional cycle contains the Upper Eocene-Oligocene, Miocene and younger section.

3. Methodology

The studied oil field will be inspected using available data in nine representative wells, for the purpose of evaluation the Safa reservoir .These wells are: (Phiops-1X, Faghur D-1X, Siwa A-1X, Siwa C-1X, Siwa F-1X, Wkal A-1X, Buchis W-1X, Tayim W-1X, Neith S-2) (Fig. 1).

4. Petrophysical analysis

4.1 M-N Cross-plot:

Lithology interpretation with neutron, density, and sonic logs is made easy by the use of M-N plots. This plot was first presented by **Bruke et al., (1969)**. It combines the data of all three porosity logs to give the lithology-dependent quantities, M and N, which are essentially independent of primary porosity. Therefore a cross-plot of these two quantities makes lithology characteristics be more apparent.

M and N are defined as:

$$M= (\Delta t_f - \Delta t) / (\rho b - \rho b_f) \times 0.01 \ldots\ldots\ldots\ldots \textbf{(1)}$$

$$N= (\phi_{nf} - \phi n) / (\rho b - \rho b_f) \ldots\ldots\ldots\ldots\ldots\ldots \textbf{(2)}$$

Where;

$\Delta t_{f:}$ Interval transit time of the mud fluid. Δt: Sonic log reading.

$\phi_{nf:}$ Neutron of mud fluid. ϕ_n: Neutron log reading.

ρb_f : Density of mud fluid. ρb : Density of mud fluid.

Quartz, limestone and dolomite are the three standard minerals composing the rock units. The arranged values of M are plotted vs. N to generate the M-N plot used for mineral identifications. The place to which the plotted points are directed relies on the different amount of matrix components they have. If it is monomineral, it will fall very close or exactly coincide on the corresponding standard points. If it has binary mixture, it will fall on the line connecting the two corresponding points. But if it has a mixture of three minerals, it will plot within the triangle formed by connecting the three respective single-mineral points.

The effect of secondary porosity, shaliness, and gas-filled porosity will raise the position of the points with respect to their true lithology, and can even cause the M-N points to plot outside the triangular area set by the primary mineral constituents. The displacement of the plotted points upward indicates secondary porosity while the effect of gas may shift the points to upwards on the right. No unique shale point exits on the M-N plot because shales tend to vary in their characteristics. Mostly, shale effect will be situated below the line that joins the silica and anhydrite points **(Bigelow, 1995)**.

Some distortion of scattered points have been identified on M-N graphs in that may be due to the presence of radioactive elements and organic matters which cases some deflections on sonic readings which affect the M-N graphs and make such these distortions **(Schlumberger 1972).** Figure (3) shows the mineralogical composition of Safa reservoir. The major of the plotted points tend to be aligned around sandstone point and slightly near limestone point but far from dolomite point. It shows the presence of sandstone

lithology with small amount of limestone matrix. Some distorted points are shifted upwardly due to secondary porosity effect. Some other points are moved downwardly due to shale effects, this effect may cause the shifting of some points near the dolomite region.

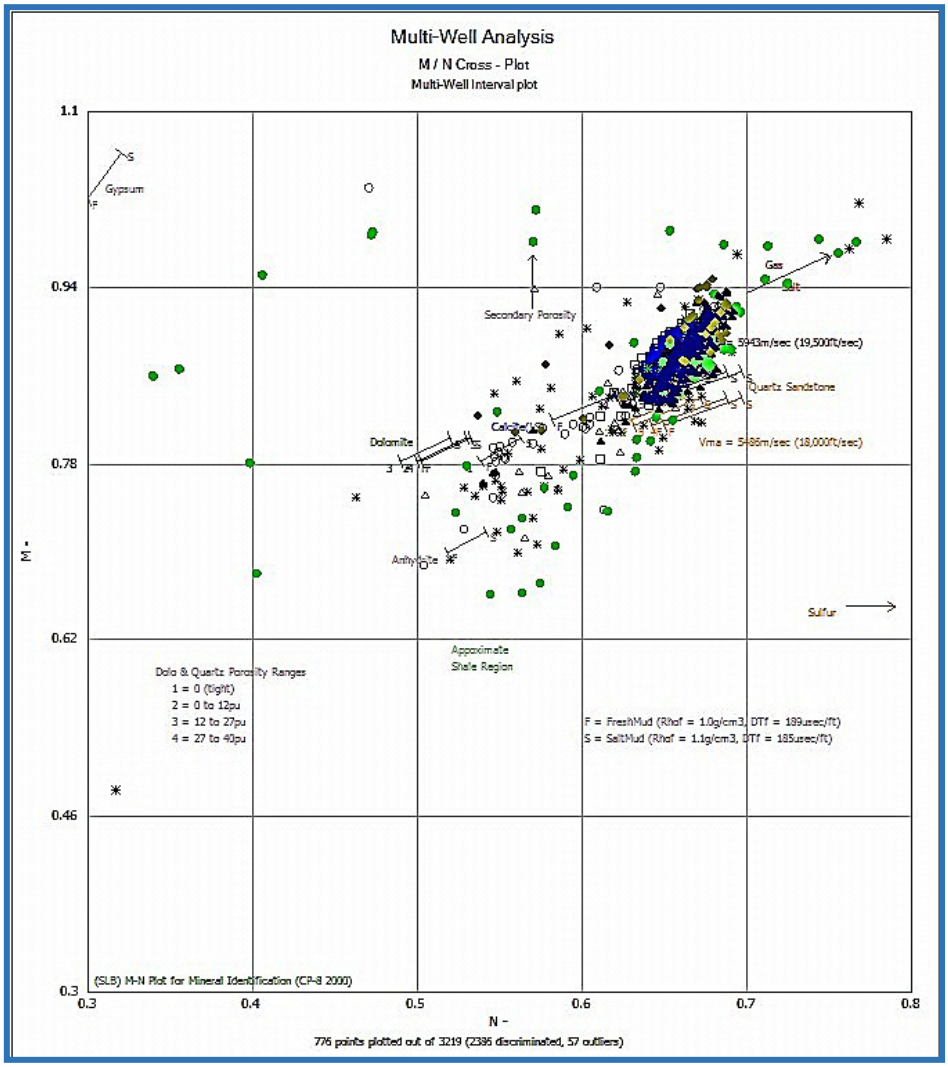

Fig. (3): M-N cross-plot of Safa reservoir, in Faghur- Siwa Basin.

4.2 Dia Porosity Cross-plot:

Figure (4) shows the neutron-density cross-plot of **Safa** reservoir, the reservoir rocks dispersed in sandstone area with minor occurrences toward limestone area due to calcareous cement, the porosity varies from 6% to 14%. The porosity indicates slight enhancement toward the west to northeast direction where SIWA C-1X, is present with porosity ranges from 14 to 16%. On the other hand the lowest porosity

values recorded toward the east direction where NEITH S-2 is present. The shifting of some points towards the dolomite line may be due to shale effect.

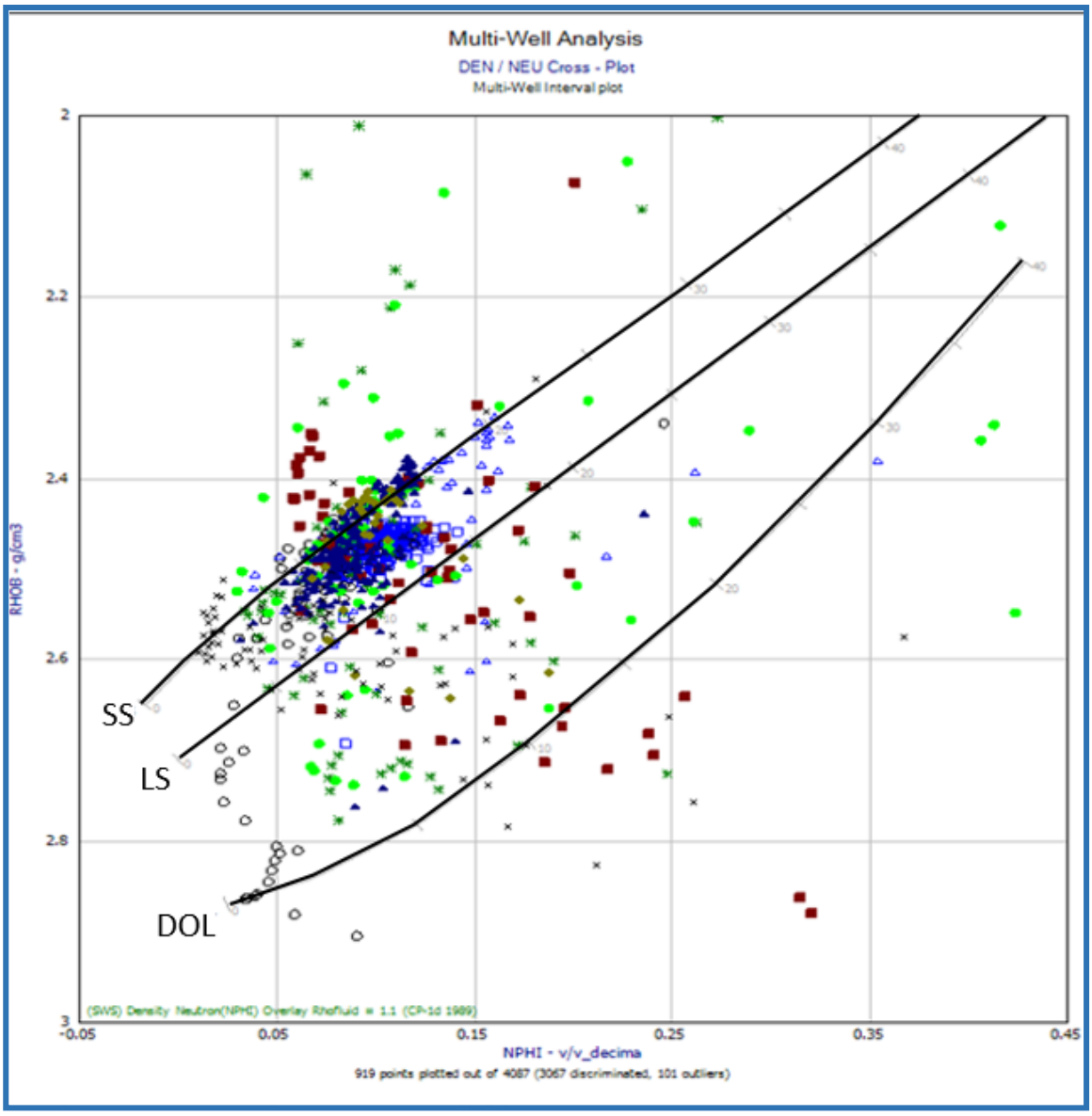

Fig. (4) Density neutron cross-plot of **Safa** reservoir, in Faghur- Siwa Basin.

4.3 Reservoir pressure measurement:

The repeat formation tester (RFT) is an open hole logs used for measuring vertical pressure distribution in a reservoir, the technique of point-by-point evaluation of reservoir pressure is used to detect pressure profiles, fluid density, fluid contacts, differential depletion and reservoir intercommunication. RFT is a device capable of providing an estimate of formation permeability through the interpretation of pretest

pressure data record during drawdown and build up (**Stewart and Wittmann, 1979**). Reservoir pressure is necessary to get acquaintance with the driving mechanisms that dominate the behavior of fluids within reservoirs.

Cole (1969) suggested that a depletion-drive reservoir can be identified by reservoir pressure: The reservoir pressure declines rapidly and continuously. This reservoir pressure behavior is attributed to the fact that no extraneous fluids or gas caps are available to provide a replacement of the gas and oil withdrawals.

Cole (1969) and Clark (1969) presented a comprehensive review of the reservoir pressure characteristic trend associated with gas-cap-drive reservoirs. The reservoir pressure falls slowly and continuously pressure tends to be maintained at a higher level than in a depletion drive reservoir. The degree of pressure maintenance depends upon the volume of gas in the gas cap compared to the oil volume.

Cole (1969) presented the following discussion on the reservoir pressure characteristic that can be used for identification of the water-driving mechanism. The reservoir pressure decline is usually very gradual. The reason for the small decline in reservoir pressure is that oil and gas withdrawals from the reservoir are replaced almost volume for volume by water encroaching into the oil zone.

Cole (1969) stated that reservoir operating largely under a gravity drainage producing mechanism are characterized by variable rates of pressure decline, depending principally upon the amount of gas conservation.

Besides the measurement of formation pressure, The RFT has found many applications in the field of reservoirs.

1) In exploration wells in unproductive fields, it is known that formation pressures must match with gravity-capillary equilibrium established over geologic times. Thus the conduct of the RFT survey and the interpretation of the data are governed by the constraint that the formation pressure lie on straight line fluid gradients. The main objective of the testing is to define these gradients (water, oil and gas) and their intersections.

2) In development wells, either partial depletion or possible water injection may already impact the observed formation pressures. Thus the new development well is used as an observation location at which the current state of the reservoir can be calculated on a vertically distributed basis.

A plot of formation pressure against depth can give valuable information of the reservoir, and it gives an indication of the nature of formation fluids (gas, oil, or water) as well as the position of the interfaces between different phases (gas-oil contact, oil-water contact) **(Stewart and Wittmann, 1979).** It should be noted that the intercept of the pressure gradients, corresponding for instance to oil and water, is representative of the so-called free water level, it may thus be somewhat below the 100% water level, as indicated by logs, due to capillary pressure effects.

Figure (5) shows the pressure data for Safa presented in phiops-1x well. Oil gradients (0.25 psi/ft. and 0.1 psi/ft.) were observed in Safa reservoir and the oil gradient (0.176 psi/ft.) in Desouqy reservoir. Generally, due to the lithology of Safa is heterogeneity from sand body with intercalation of shale and siltstone streaks, so it is difficult to determine oil water contact. Finally Safa reservoir is considered as partial water drive due to pressure decrease from 6270 psi to 6060 psi.

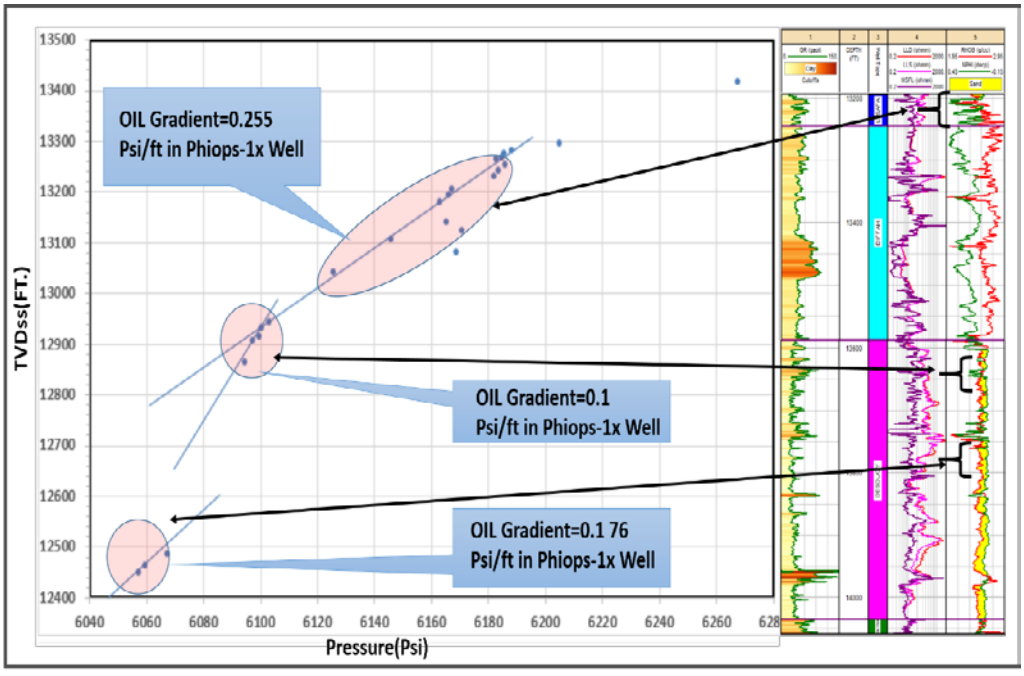

Fig. (5) Analysis of Safa reservoir pressure data (RFT), in Phiops-1x

4.4 Lateral Variation of Petrophysical Characteristics of Safa Reservoir

4.4.1 Shale volume

The shale volume distribution map for Safa reservoir shows that it increases toward the southwest and the north directions, which is related to facies distribution affected by transgressive system tract (TST), where the porosity and the net-pay increase toward the west and the northeast directions. It reaches the maximum value (16%) at SIWA F-1X, and decreases towards the east and the south directions of the area due to low stand system tract (LST), to reach (2%) as a minimum value at NEITH S-2, BUCHIS W-1X wells Figure (6).

4.4.2 Net pay

The net pay distribution map shows an increasing toward the west direction. It reaches the maximum value (46 ft.) at FAGHUR D-1X. Where the water saturation increases toward the southwest and the central part of the study area.

It shows observed decreasing toward the east and the south directions to reach zero value SIWA A-1X, SIWA C-1X, and BUCHIS W-1X wells as illustrated in Figure (7).

4.4.3 Effective porosity

The effective porosity distribution map for Safa reservoir in Faghur- Siwa Basin shows an increasing towards the west and the northeast directions, which is related to facies distribution affected by low stand system tract (LST), where it reaches (13%) at SIWA C-1X well. On the other hand, it decreases towards the east and the south directions to reach (7%) as a minimum value at NEITH S-2 well Figure (8).

4.4.4 Water saturation

The water saturation distribution map for Safa reservoir in Faghur- Siwa Basin shows that it increases toward the southwest and the central part directions which is related to structural control, where it reaches the maximum value (95%) in both SIWA

A-1X and BUCHIS W-1X wells. It reaches the minimum value (9%) toward the west direction in both FAGHUR D-1X, TAYIM W-1X wells (Fig.9).

4.4.5 Hydrocarbon saturation

The movable hydrocarbon saturation map of SAFA reservoir Figure (10) illustrates a decreasing toward the south and the central part directions where it reaches the minimum value (15%) at SIWA A-1X and BUCHIS W-1X wells.

The increasing is observed toward the northwest direction, which is related to structural control (Step faults) and facies distribution, where the maximum value was (75%) at TAYIM W-1X well.

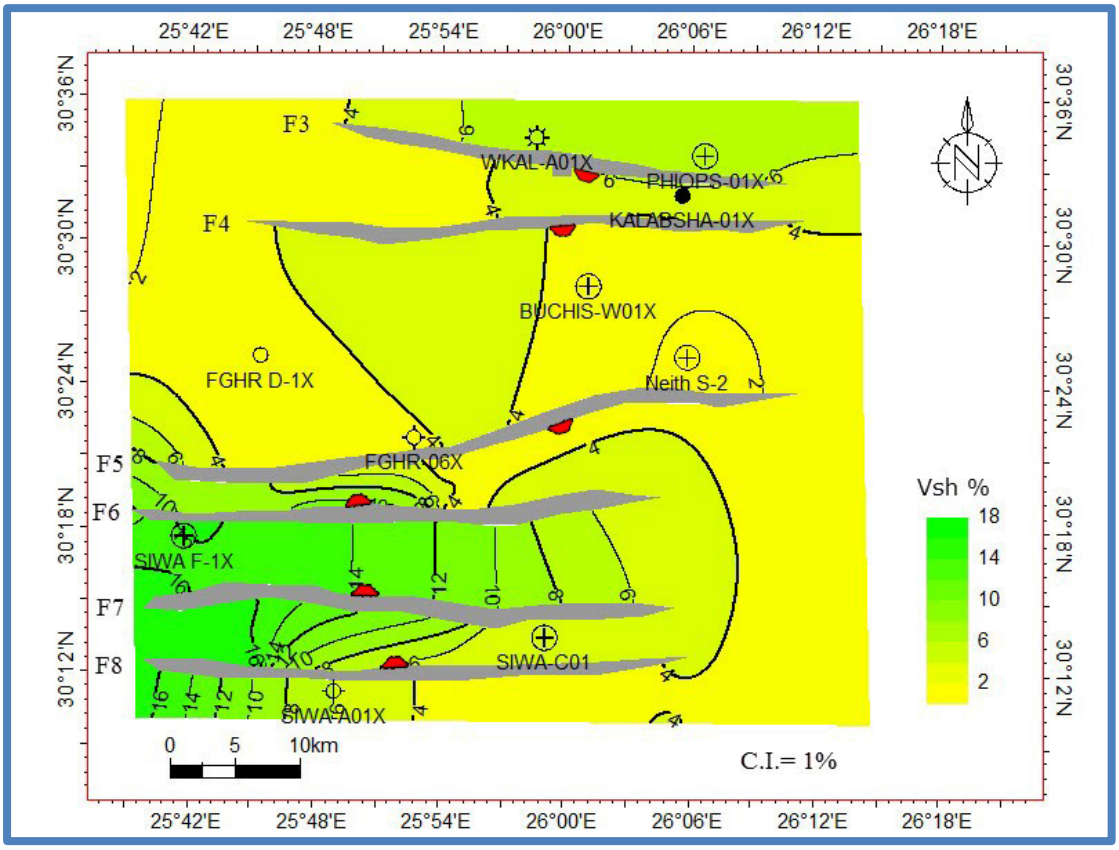

Fig. (6) Shale volume map of **Desouqy** reservoir in Faghur-Siwa Basin.

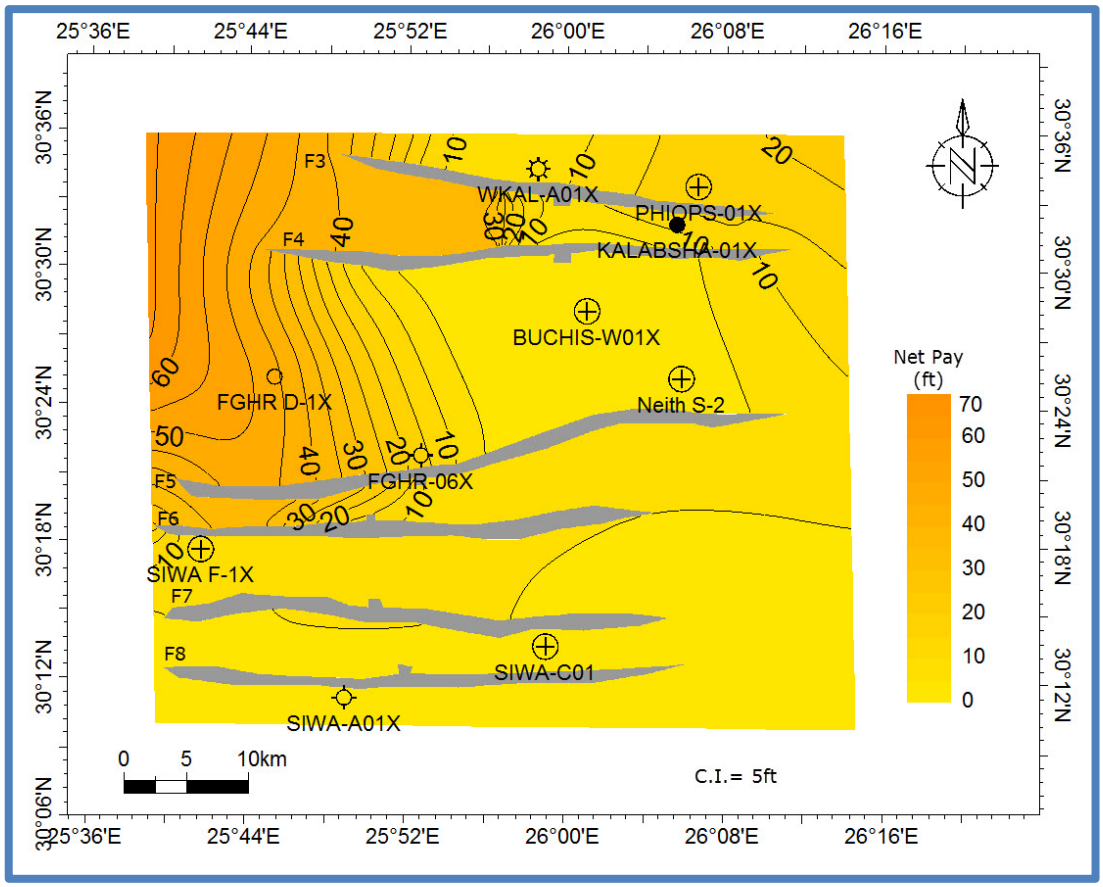

Fig. (7) Net pay map of **Safa** reservoir in Faghur-Siwa Basin.

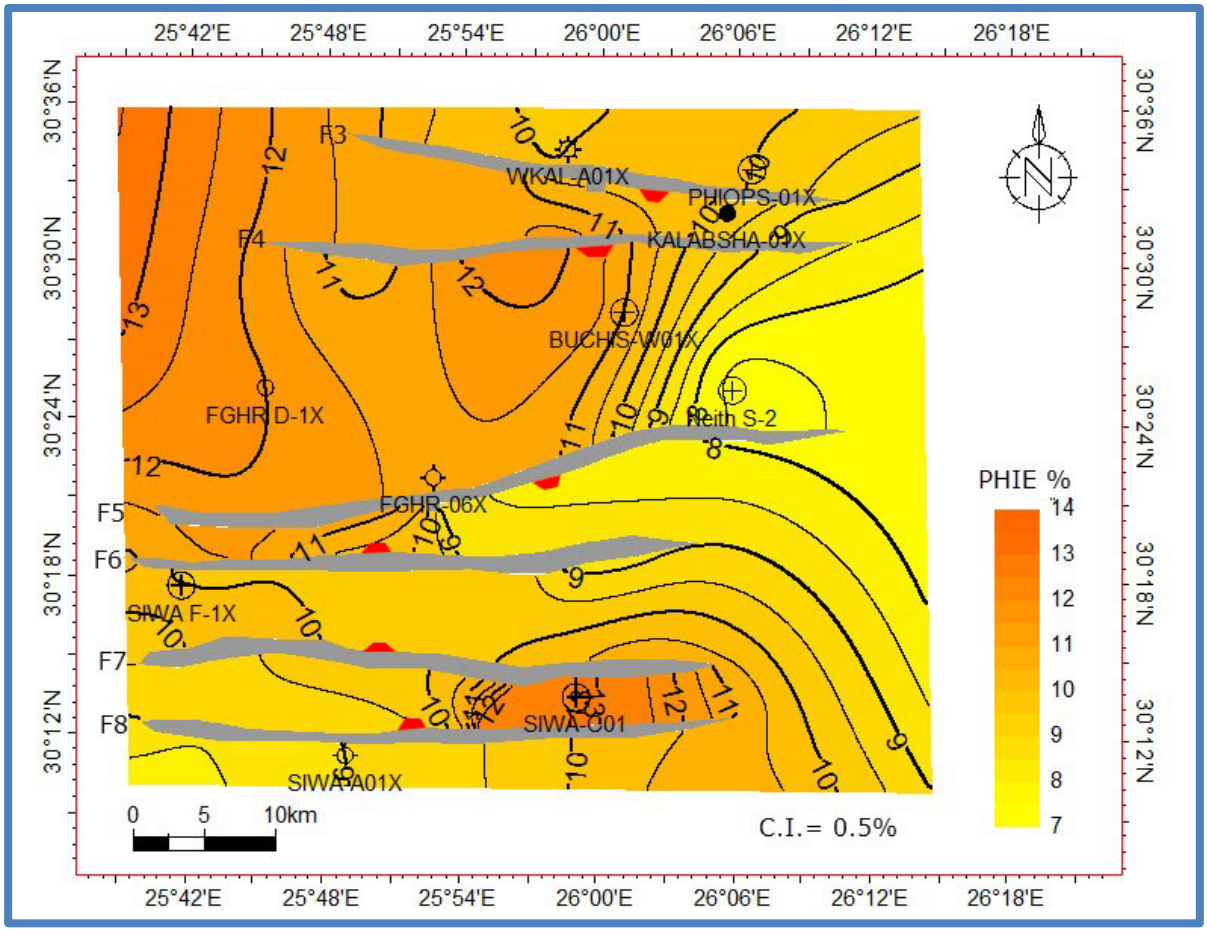

Fig. (8) Effective porosity map of Safa reservoir in Faghur Siwa Basin.

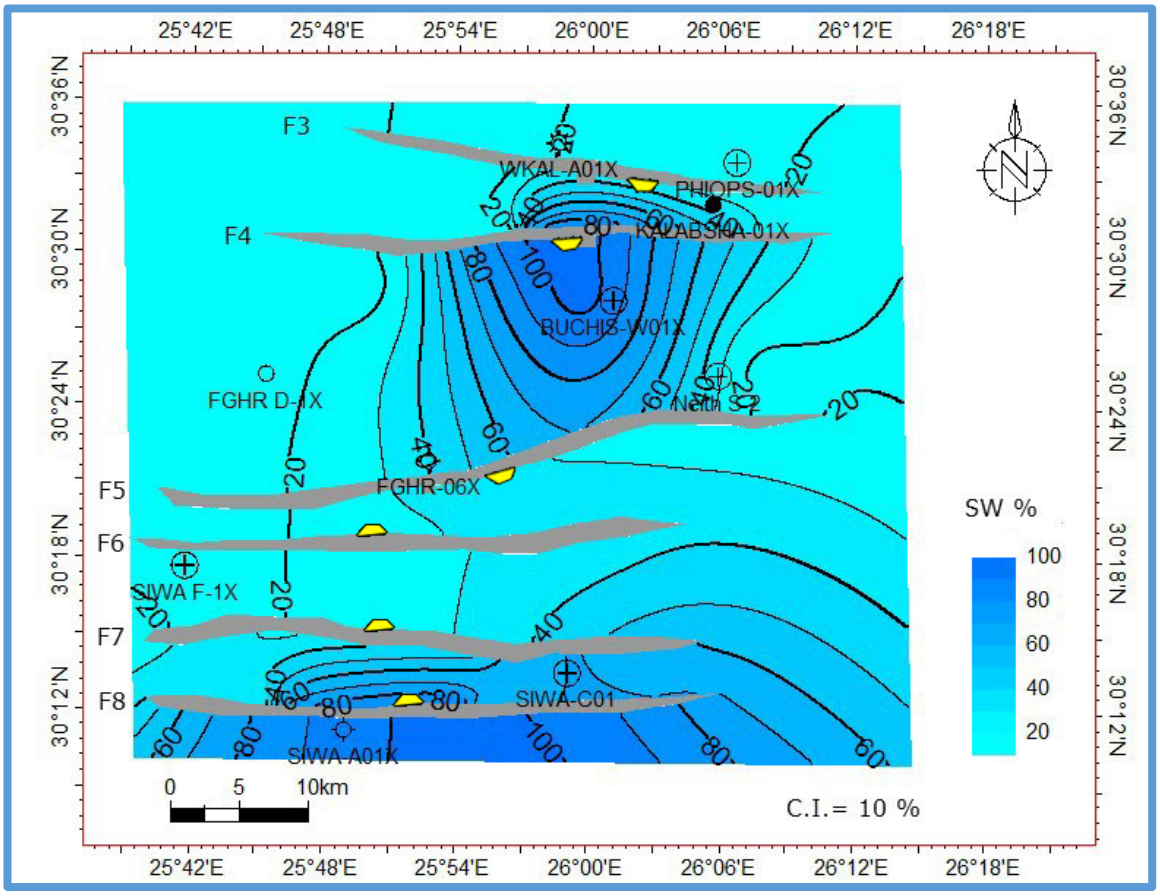

Figure (9) Water saturation map of Safa reservoir in Faghur Siwa Basin.

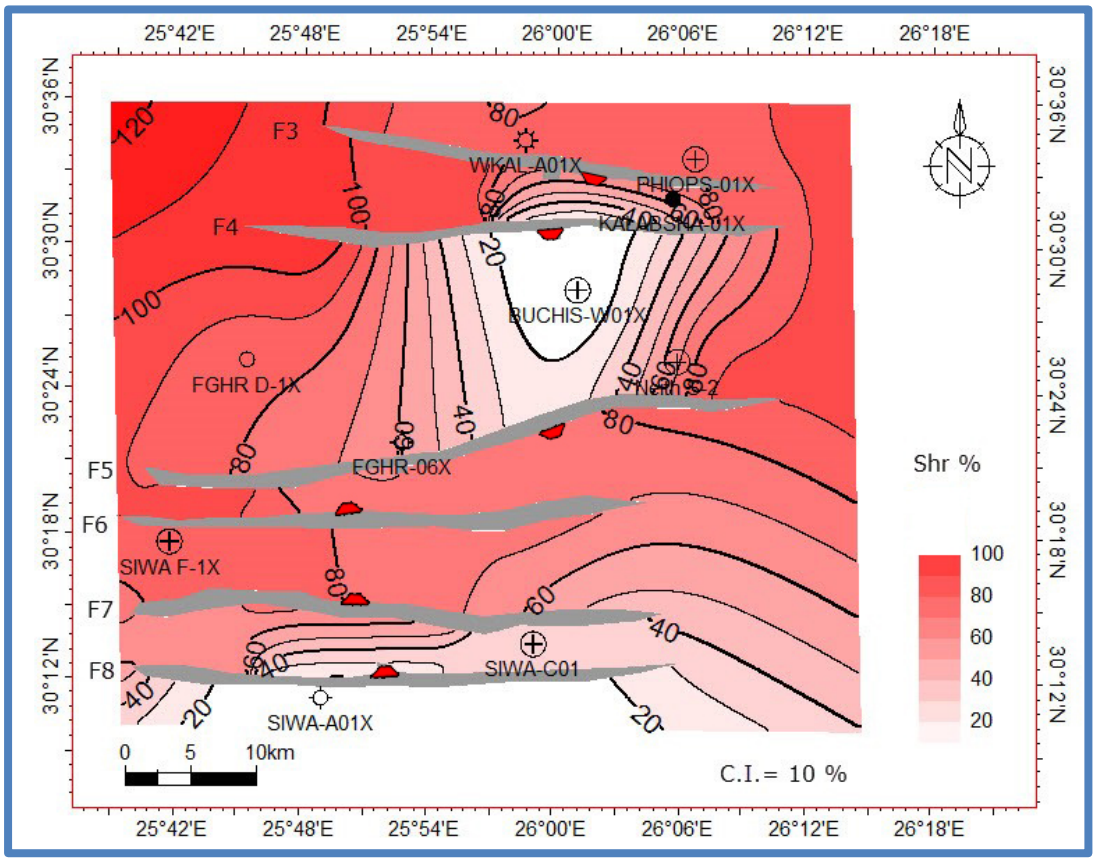

Fig. (10) Movable Hydrocarbon saturation map of Safa reservoir in Faghur-Siwa Basin.

4.5 Vertical Variation of Petrophysical Characteristics

Figure (11) shows that the vertical distribution of hydrocarbon occurrences can be explained and presented through the construction of the litho-saturation cross-plots. The litho-saturation cross-plots of Safa Formation show the predominance of sandstone in the top L. Safa due to the regressive cycle .Also, It shows that, The shale content ranges between (3%-16%), and the effective porosity ranges between (6%-13%), While the hydrocarbon saturation is about (85%).Where the sedimentation resumed during the Jurassic as a response of subsidence connected with the opening of the Tethyan Sea. This extensional event locally caused the re-activation of the pre-existing E-W faults.

The result of relation among E-W fault directions initiated the step fault blocks and graben gave rise to varying structural closures. These closures formed good sites for the entrapment of hydrocarbons.

4.5.1 Correlation Charts

The aim of correlation chart is to follow the changes in lithologic characters or any break in the depositional continuity. It shows the equivalency of stratigraphic units, and to exhibit thickness variation.

The first correlation chart (B-B') extends in N-S directions and passing through Phiops-1x, Neith S-2 and Siwa C-1 wells Figure (12). The correlation chart shows that the Safa S1 unit is represented in this section in all wells but with different variety, where the thickness in Phiops-1x is more than the other wells. The Safa R1 is a thin layer in Phiops-1x well, but reduced in the other wells.

The second correlation chart (D-D') extends in W-S directions and passing through Siwa F-1X, Siwa A-1X and Siwa C-1X wells Figure (13). The correlation chart shows that the Safa S1 unit has a great thickness in Siwa F-1X well more than the other wells, the Safa R1 reservoir is a thin layer has a little thickness in Siwa F-1X well decreased in Siwa A-1X and Siwa C-1X wells.

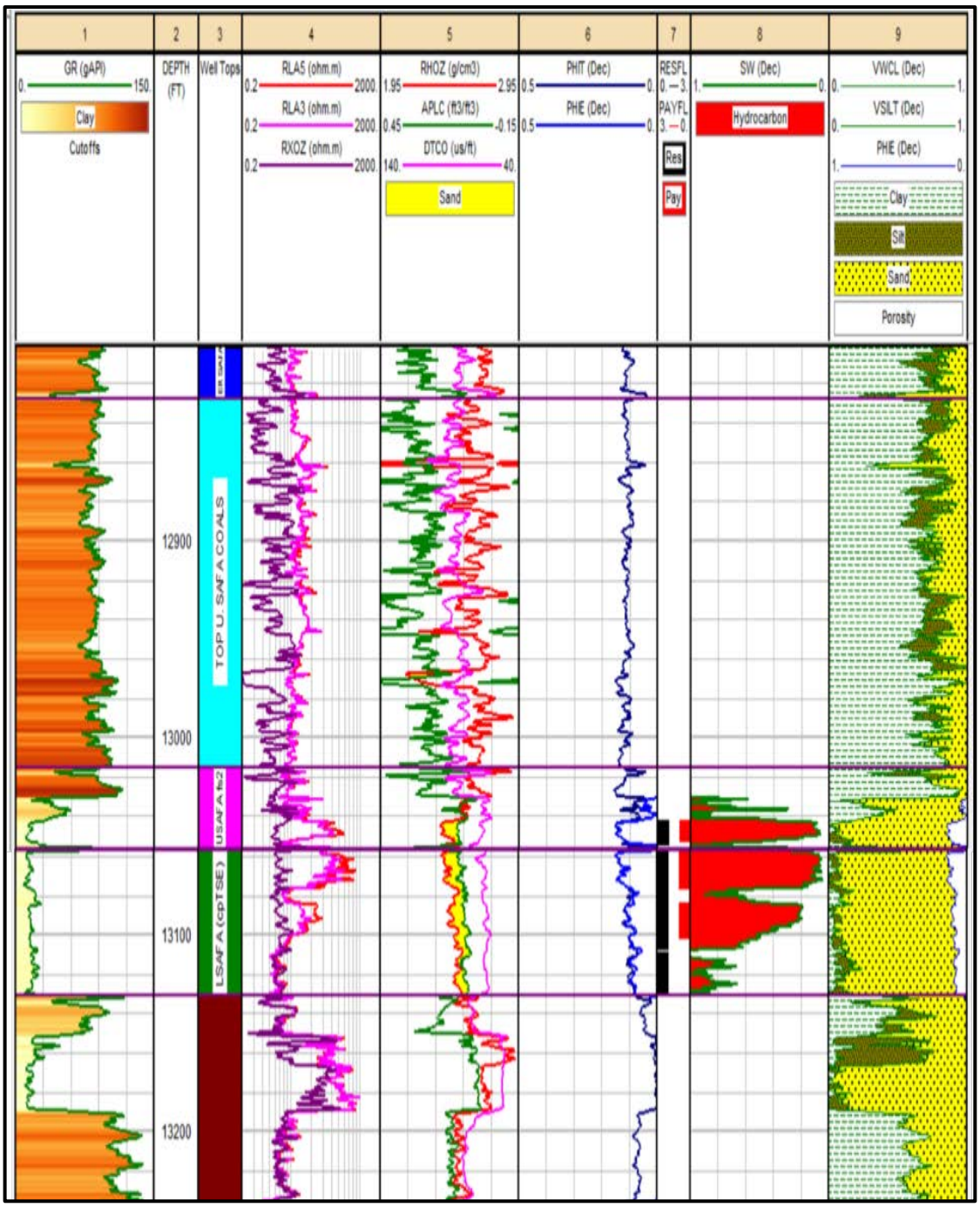

Fig. (11): Computer processed interpretation (CPI) plot for the Safa reservoir in Faghur-Siwa Basin.

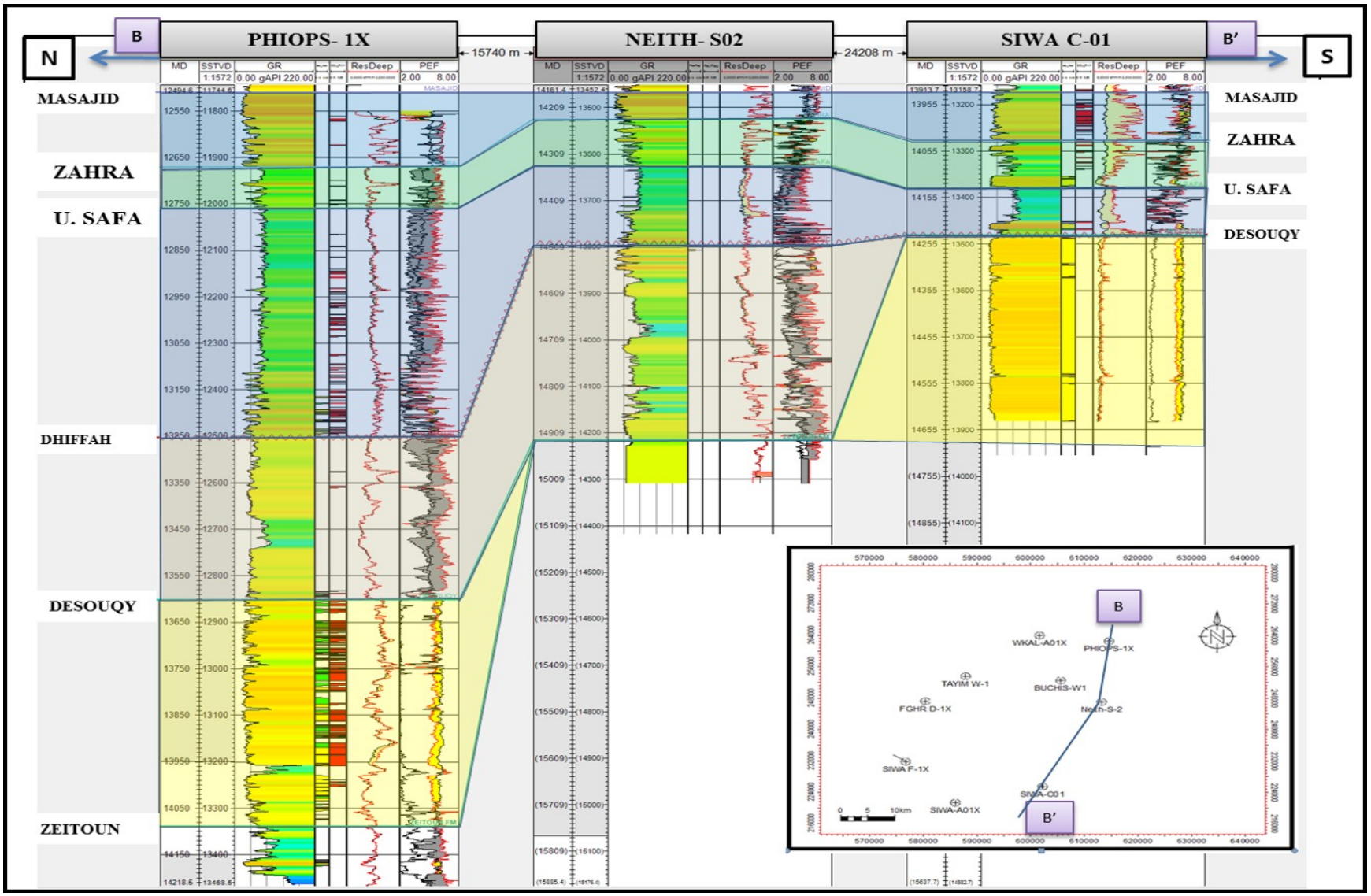

Fig. (12) Correlation chart along the profile (B-B')

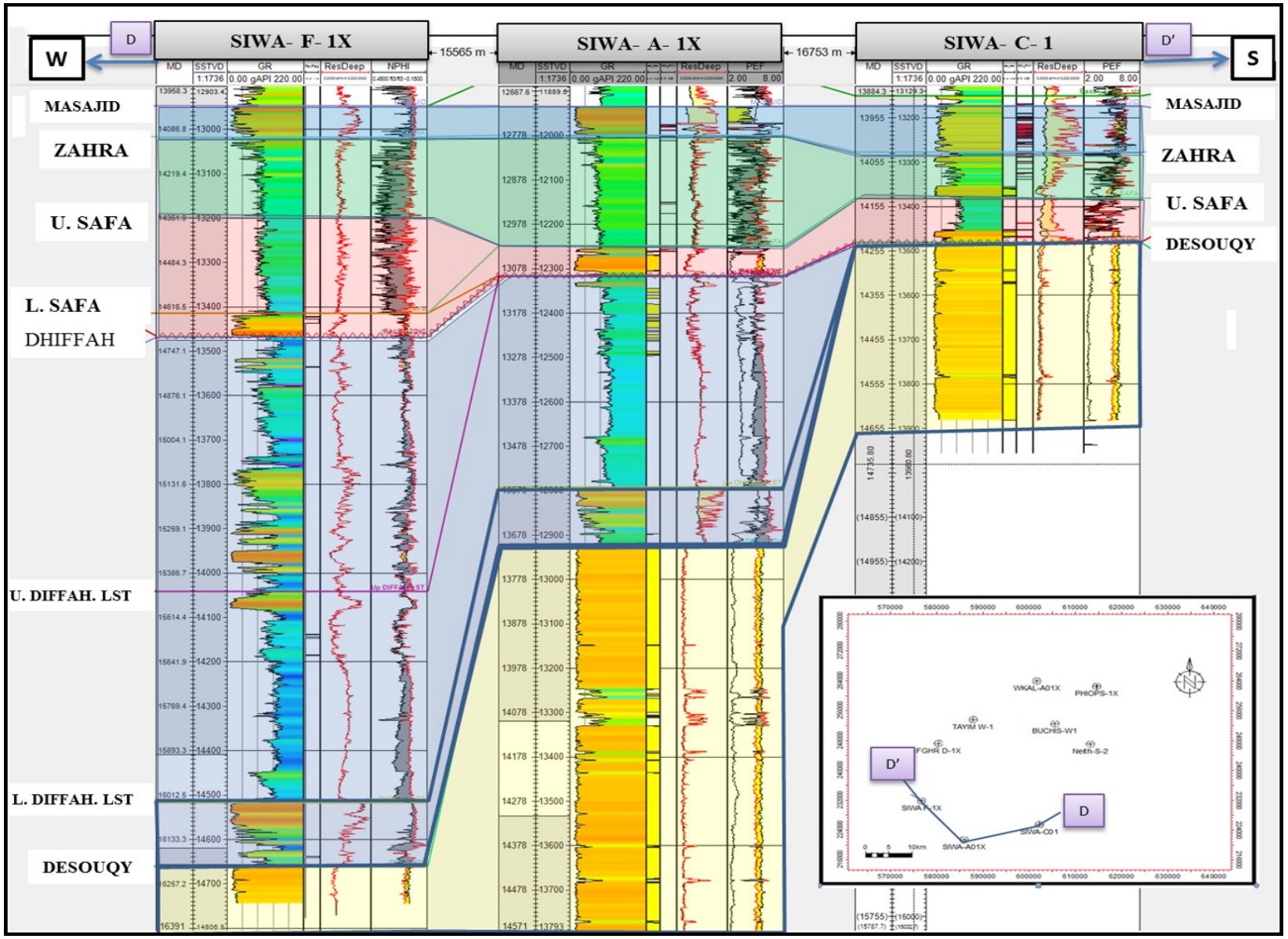

Fig. (13) Correlation chart along the profile (D-D')

4.6 Structural map on the top of Safa Formation

The time reflection map delineated on the top of the Permian age. Figure (14) reveals an irregular distribution pattern with maximum value of 2800 msec (structurally low), at the southeastern and the central parts of the study area respectively. On the other hand, the time decreases on the uplifted footwall of the faults on the area, recording values 1800 msec (structurally high) at the northern part of the study area. The basin trend at southeastern part of study area. The major strikes E-W trends, this group during (Cambrian- Devonian) related to Caledonian to (Turonian- Santonian) related to Sub-Hercynian - Early Syrian Arc. This trend was emphasized in seismic section in figure (15).

The result of relation among E-W fault directions initiated step fault blocks and graben gave rise to varying structural closures. These closures formed good sites for the entrapment of hydrocarbons.

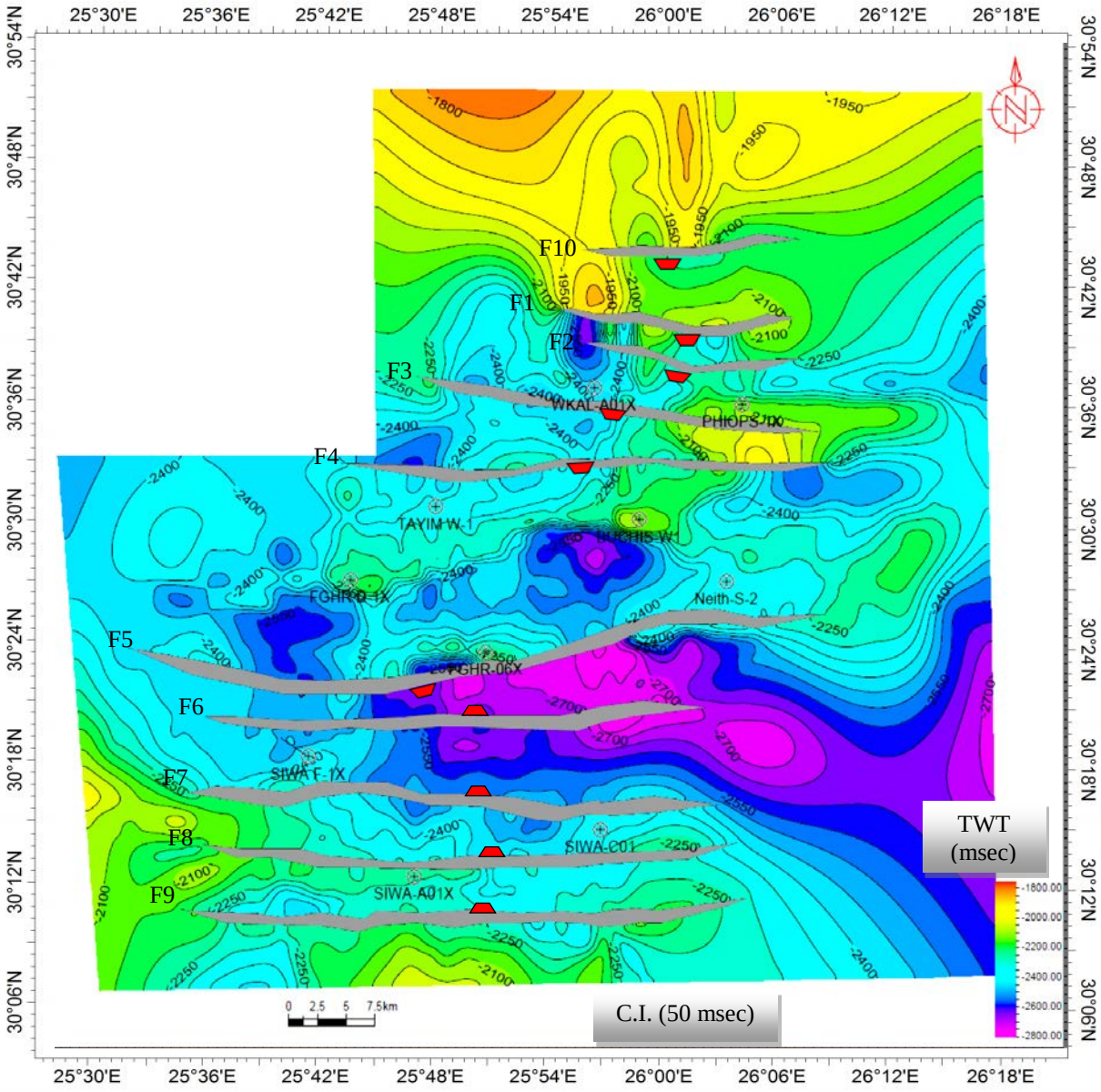

Fig. (14): Two-way time structural contour map on the top of Safa Formation in Faghur and Siwa basin.

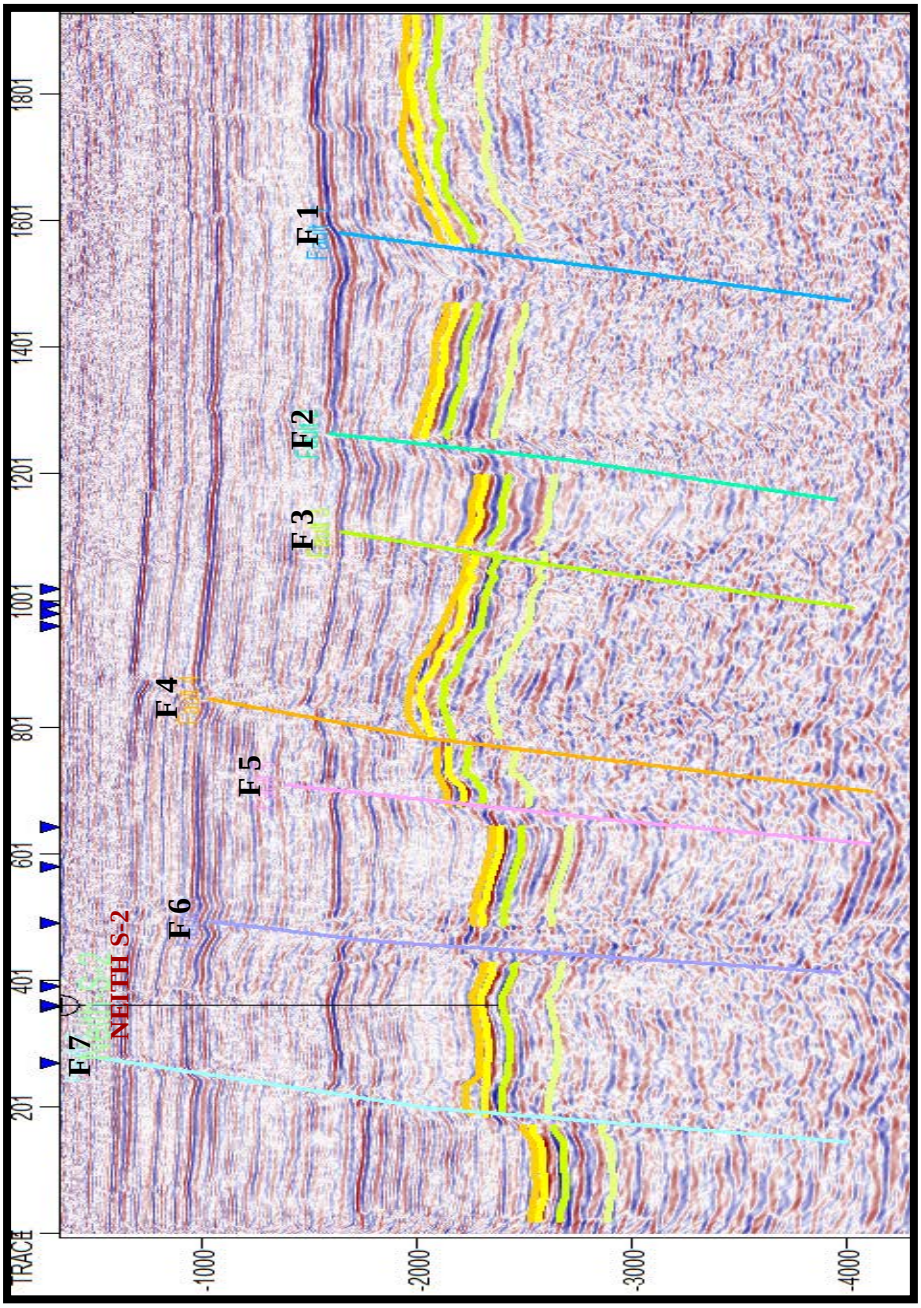

Fig. (15) Seismic interpretation of the E-W seismic line showing faults trend.

Relationship between effective porosity from log and fluid porosity from core of Safa reservoir in Phiops-1X well:

From the relationship between effective porosity from log and fluid porosity from core of Safa in Phiops-1x well are shown in figure (16).

The following results are obtained from core analysis.

In Phiops -1x well, The high stander deviation values 2.79 % for helium porosity these indicate that, the Safa reservoir has a heterogeneous porosity values and the statistical analysis for the porosity values ensuring that, the Safa reservoir is represented by fair reservoir.

From the relationships between helium porosity and permeabilities of Safa in Phiops-1x well.

From this figure, we can note that the correlation coefficients for this relationship is 0.919 for both fluid porosity and effective porosity. We can conclude that Safa reservoir is a fair reservoir in Phiops-1X well.

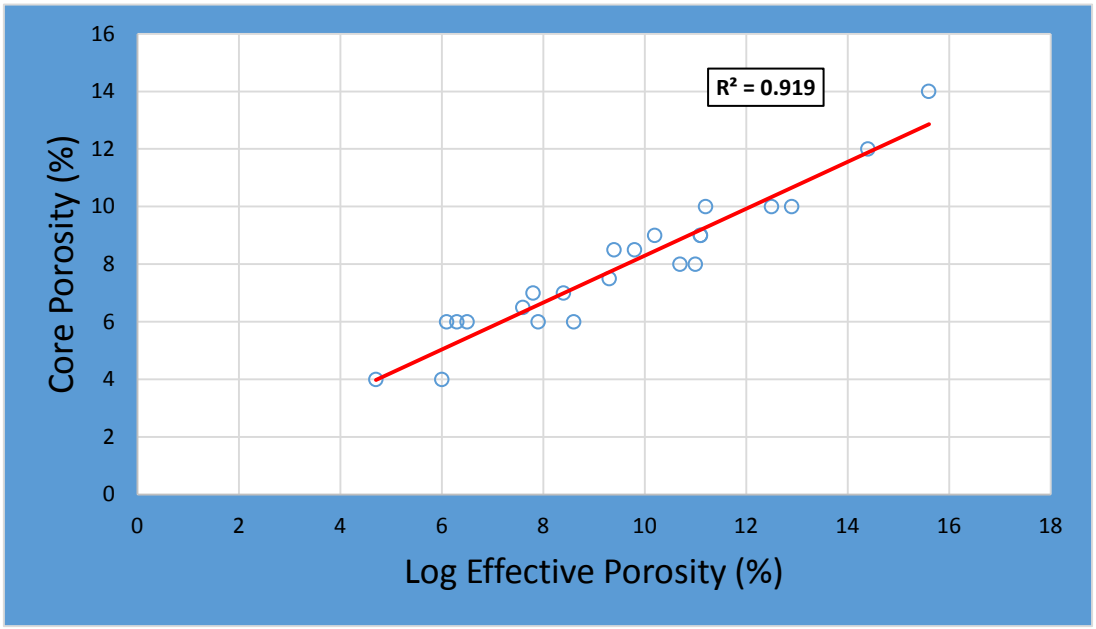

Fig. (16) Relation between effective porosity from log & fluid porosity from core of the Safa reservoir in Phiops-1x well.

Conclusion

The petrophysical characteristics of the Safa Formation show that, the shale content (V_{SH}) increases towards the southwest and the central part directions where it achieves the upper limit value (15.8%) at SIWA F-1X, and falls towards the west direction to reach (1.2%) as a lower limit value at NEITH S-2, BUCHIS W-1X wells.

The effective porosity (Φ_{eff}) is increasing towards the north western and the south-central directions where it reaches (12.9%) at SIWA C-1X well.

On the other hand, it falls towards the east direction to reach (6.5%) as a lower limit value at NEITH S-2 well. and S_{hr})

The hydrocarbon saturation (S_{hr}) is decreasing towards the east and central part directions where it passes the minimum value (4.9%) at SIWA A-1X and BUCHIS W-1X wells. The increasing is observed towards the north western and the south-central directions where the upper limit value was (90%) at TAYIM W-1X well.

M-N cross-plots for mineralogical composition of the Safa reservoir show that, the bulk of the plotted points tend to align around sandstone point and slightly near limestone point but far from dolomite point. It may suggest the presence of sandstone lithology with small quantity of limestone matrix. Some distorted points are shifted upwardly due to secondary porosity effect. Some other levels are shifted downwardly due to shale effects, this result may cause the switching of some peaks near the dolomite region.

The best reservoir characteristics of Safa reservoir occur in the northwestern and south-central parts attaining high effective porosity, low water saturation and shale content.

The source facies are expected to occur in the basinal areas between F6, F7 and F5 (graben blocks). The hydrocarbons are assumed to be generated within the basinal areas and then migrated to the step fault blocks of the northwestern sector between F5 and F4 and the south-central sector between F6 and F7 faults. So, faults F5 and F6 are expected to represent leaking faults.

The analysis of reservoir pressure data of Safa reservoir in Phiops-1x, indicates that, the oil gradients (0.25 psi/ft. and 0.1 psi/ft) were observed in Safa reservoir. Generally, due to the lithology of Safa is heterogeneity from sand body with intercalation of shale and siltstone streaks, so it is difficult to determine oil water contact. Finally Safa reservoir is considered as partial water drive due to pressure decrease from 6270 psi to 6060 psi.

The result of relation among E-W fault directions initiated step fault blocks and graben raised varying structural closures. These closures formed good sites for the entrapment of hydrocarbons.

As a result of the present study, using the subsurface and petrophysical evaluation, it is advised to drill prospect wells in the northwest and the south-central part in the area under investigation to drain the oil from the extended reservoirs expected to be above OWC.

Also, it is recommended to cover the area by 3D seismic acquisition to enhance the seismic data.

References

Bigelow, L., 1995: Introduction to Wireline Log Analysis, Western Atlas International, Inc., Houston, Texas-USA.

Bruke, J.A.; Campbell, R. L.; and Schmidt, A. W., 1969: "The litho-porosity crossplot". The log analyst (SPWLA) Vol. 10 No. 6. 302

EGPC (Egyptian General Petroleum Corporation), 1992: Western Desert, oil and Gas fields, a comprehensive overview. EGPC, 11th Petrol. Expl. and Prod. Conf., Cairo, 431p

Cole, F., 1969: Reservoir Engineering Manual. Gulf Publishing Co., Houston.

Said, R., 1990: Cretaceous paleogeographic maps. In Said, R. (ed.). The Geology of Egypt. Balkema-Rotterdam-Brook field. pp. 439-449.

Schlumberger, 1972: The essential of log interpretation practice. Schlumberger Ltd., France, pp 45-67.

Schlumberger, 1995: Well Evaluation Conference, Egypt. Schlumberger Technical Editing Services, Chester. pp. 58-66.

Stewart, G., and Wittmann, M. J., 1979: Interpretation of pressure response of the repeat formation tester, SPE, fall meetings in Las Vegas, 10181 p.